

Article Draft

A double-sampling extension of the German National Forest Inventory for design-based small area regression estimation of timber volume resources on forest district levels

Large scale application to the federal state of Rhineland-Palatinate

Andreas Hill^{*†}, Daniel Mandallaz^{*}, Joachim Langshausen^{**}

^{*}Department of Environmental Systems Science, ETH Zurich
^{**}Forest Service Rhineland-Palatinate

Corresponding author[†]: andreas.hill@usys.ethz.ch
Co-authors: daniel.mandallaz@env.ethz.ch, joachim.langshausen@wald-rlp.de

Publication date: February 2, 2018

Abstract

The German National Forest Inventory consists of a systematic grid of permanent sample plots and provides a reliable evidence-based assessment of the state and the development of Germany's forests on national and federal state level in a 10 year interval. However, the data have scarcely been used for estimation on smaller management levels such as forest districts due to insufficient sample sizes within the area of interests and the implied large estimation errors. In this study, we present a double-sampling extension to the existing German National Forest Inventory (NFI) that allows for the application of recently developed design-based small area estimation procedures that try to overcome the restriction in terrestrial sample size by enlarging the sample by a large set of model predictions. We illustrate the implementation of the estimation procedure and evaluate its potential by the example of timber volume estimation on two small scale management levels (42 and 392 forest district units respectively) in the federal German state of Rhineland-Palatinate. A LiDAR derived canopy height model and a tree species classification map based on satellite data were used as auxiliary information in an ordinary least square regression model to produce the timber volume predictions on the plot level. The results indicate that the suggested double-sampling procedure can significantly increase estimation precision on both management levels compared to estimates based on the simple random sampling (SRS) estimator: on Forstamt-level, the proportion of estimation errors below 6% could be increased from 10% to 60% (90% were below 7% estimation error). The increase of estimation precision was even more pronounced on the Revier-level, although the errors were generally higher than on the Forstamt-level: here, the proportion of estimation errors below 10% could be increased from 15% to 40%. The average decrease in variance was ... and ..., and the relative efficiency was ... and ... on Forstamt and Revier-level respectively.

Keywords. National forest inventory, small area estimation, double sampling for regression within strata, cluster sampling, LiDAR canopy height model, tree species classification

Contents

1	Introduction	1
2	Terrestrial sampling design of the German NFI	4
3	Double sampling in the infinite population approach	4
4	Estimators	5
4.1	Design-based SRS estimator for cluster sampling	5
4.2	Design-based small area regression estimators for cluster sampling	7
4.2.1	Pseudo Small Area Estimator (<i>PSMALL</i>)	7
4.2.2	Pseudo Synthetic Estimator (<i>PSYNTH</i>)	9
4.2.3	Extended Pseudo Synthetic Estimator (<i>EXTPSYNTH</i>)	9
4.3	Measures of estimation accuracy	10
5	Case study	11
5.1	Study area and small area units	11
5.2	Terrestrial sample	11
5.3	Extension to double sampling design	12
5.4	Auxiliary information	13
5.4.1	LiDAR canopy height model	13
5.4.2	Tree species map	14
5.5	Calculation of the auxiliary variables	16
5.5.1	LiDAR canopy height model	16
5.5.2	Tree species map	16
5.6	Regression Model	17
5.6.1	Design-Based Model Inference	17
6	Results	18
6.1	General estimation results	18
6.2	Estimation errors	19
6.3	Comparison of <i>PSMALL</i> and <i>EXTPSYNTH</i>	20
6.4	Reduction of variance by two-phase estimators	21

List of Figures

1	<i>Left:</i> Study Area with delineated FA forest management units. <i>Right:</i> Example for each of the three management units (from top to bottom): FA, FR and forest stand unit with overlayed the extended double sampling cluster design. <i>Green:</i> Forest stand polygon layer defining the forest area of this study.	12
2	Left: CHM (top) and tree species classification map (bottom) available on the federal state level were used as auxiliary information. Right: Magnified illustration of the rectangular supports used to derive the explanatory variables from the auxiliary information.	15
3	Cumulative distribution of estimation errors under the simple random sampling (SRS), the pseudo small (<i>PSMALL</i>), the extended pseudo synthetic (<i>EXTPSYNTH</i>) and the pseudo synthetic (<i>PSYNTH</i>) estimator. <i>Left:</i> Results for the 45 FA units. <i>Right:</i> Results for the 388 (SRS), 321 (<i>PSMALL / EXTPSYNTH</i>) and 403 (<i>PSYNTH</i>) FR units.	19
4	<i>Left:</i> Comparison of the g-weight variance between the <i>PSMALL</i> and the <i>EXTPSYNTH</i> estimator for the 321 FR units. <i>Right:</i> Difference in g-weight variance between the <i>PSMALL</i> and the <i>EXTPSYNTH</i> estimator in dependence of the terrestrial data ($n2G$) in the FR unit.	20
5	Cumulative distribution of variance reduction by the <i>PSMALL</i> and <i>EXTPSYNTH</i> compared to the SRS estimator for the 45 FA and 321 FR units.	21
6	21

List of Tables

1	Descriptive statistics of the forest observed on NFI sample plots located within communal and state forest area (n=5791).	13
2	Sample size for each phase in entire study area. $n_{\{1,2\},plots}$: number of plots. $n_{\{1,2\}}$: number of cluster	14
3	Classification accuracies of the <i>treespecies</i> variable before and after calibration. n_{ref} : number of terrestrial reference plots. n_{class} : number of classified plots.	17

1 Introduction

The German National Forest Inventory (NFI) provides reliable evidence-based and accurate information of the current state and the development of Germanys forest over time. The NFI thereby has to satisfy various information needs and amongst others reports to public and state forestry administrations, wood-based industries and the public on the national level, as well as to the Food and Agriculture Organization of the United Nations (FAO) and United Nations Framework Convention on Climate Change (UNFCCC) on the international level ([Polley et al, 2010](#)). At the current time, the inventory design of the German NFI solely rests upon a terrestrial cluster inventory that is carried out at sample locations systematically distributed over the entire forest state area of Germany. As this implies covering a large area of 114'191 ha ([Thünen-Institut, 2014](#)), the sample size has been chosen according to satisfy high estimation accuracies for forest attributes on the national and federal state level. This however leads to very low sampling intensities and consequently, sample sizes often drop dramatically when entering spatial units below the federal state level. This is particularly true for forest management levels such as forest districts for which the estimation uncertainties turn out be unacceptably large due to the very limited number of sample plots within these units. For this reason, the German NFI data have not yet been extensively incorporated in operational forest planning on forest district management levels. In most German federal states, management strategies are thus still based on expert judgements from time-consuming standwise inventories (SFI), which are prone to systematic deviations [Kuliešis et al \(2016\)](#) and do not provide any measure of uncertainty.

Some German federal states, such as Lower Saxony, have approached this problem by establishing a regional Forest District Inventory (FDI) with a much higher sampling density than used by the NFI in order to base their regional management strategies on quantitative and accurate information ([Böckmann et al, 1998](#)). However, such FDIs are cost-intensive and, facing increasing restrictions in budget and staff resources, there has been a need for more cost-efficient inventory methods ([von Lüpke, 2013](#)). One method which has proven to be efficient is double-or two-phase sampling ([Särndal et al, 2003; Gregoire and Valentine, 2007; Köhl et al, 2006; Mandallaz, 2008](#)). Double sampling incorporates inexpensive auxiliary information and can be used to either increase estimation precision under given terrestrial sample size, or maintain estimation precision under reduced terrestrial sample size. A double sampling for stratification procedure has e.g. been used in the FDI of Lower Saxony ([Saborowski et al, 2010](#)), and [Grafström et al \(2017\)](#) lately illustrated how to use the auxiliary information to determine optimised balanced terrestrial sample designs. Recent studies have lately extended double-sampling to triple-sampling estimation methods using auxiliary information in two different sampling intensities. An example can be found in [von Lüpke et al \(2012\)](#) who illustrated an extension of the existing two-phase FDI Lower Saxony to a three-phase design that uses updates of past inventory data as additional auxiliary information and allows for a significant reduction of the terrestrial sample size in intermediate inventories. An other example is [Massey et al \(2014\)](#) who developed a triple-sampling extension based on the ideas of [Mandallaz \(2013b\)](#) for the Swiss NFI that can significantly reduce the increase in estimation uncertainty caused by the new annual inventory design.

1. INTRODUCTION

Two-phase and three-phase samplings techniques have also been used in the service of small area estimation (SAE). SAE techniques particular address the situation where the number of samples within a subunit, so-called small area (SA), of the entire sampling frame is too small to provide reliable estimates for that unit. A broad range of SA estimators used in forest inventories ([Köhl et al, 2006](#)) originally comes from official statistics. A commonly applied SAE method is thereby known as indirect estimation ([Rao, 2015](#)), where statistical models are used to convert auxiliary information into predictions of the target variable that is rarely or not available in the small area. The statistical models are thereby often developed by "borrowing strength" from data outside the small area. There are numerous applications of SAE in forestry ([Breidenbach and Astrup, 2012](#); [Goerndt et al, 2011](#); [Steinmann et al, 2013](#); [Mandallaz et al, 2013](#)), and most of the studies use unit-level models, i.e. the statistical models are fitted using data from inventory plots. Especially unit-level models for timber volume estimation under the use of various remote sensing data have been intensively investigated with respect to timber volume prediction ([Koch, 2010](#); [Naesset, 2014](#)). There are also few studies that have investigated area level-models, where the auxiliary information is only provided on the SA-level ([Magnussen et al, 2017](#)). Some studies have illustrated that even NFI data of low sampling densities can be used in small area estimation procedures to provide estimations of acceptable accuracy on much smaller management levels. One example is [Breidenbach and Astrup \(2012\)](#) who used data from the Norwegian NFI for SAE estimations of standing timber volume for 14 municipalities where the number of NFI samples within these areas were between 1 and 35. Estimation errors under the applied model-based and design-based SAE estimators turned to be markedly smaller than achieved under simple random sampling (SRS). Another example is [Magnussen et al \(2014\)](#) who recently used the Swiss NFI data for SAE estimation of timber volume within 108 Swiss forest districts with sample sizes between 9 and 206. Despite these promising results, a similar study in Germany using the German NFI data for SAE estimation has not yet been conducted.

The aim of this study was to investigate whether the German NFI data can provide acceptable estimation precision on two forest district levels when incorporated in small area estimation procedures. We therefore conducted a study in the German federal state Rhineland-Palatinate where we extended the German NFI to a double-sampling design and applied three types of design-based small area regression estimators in order to derive point and variance estimates of mean standing timber volume for 42 and 392 forest districts respectively. The SA-estimators we considered were the *pseudo-small*, *extended pseudo-synthetic* and the *pseudo-synthetic* design-based small area estimator suggested by [Mandallaz \(2013a\)](#); [Mandallaz et al \(2013\)](#). Auxiliary information were obtained from a countrywide airborne Laser scanning (LiDAR) canopy height model (CHM) and a tree species classification map and used for regression within tree species strata. The estimation accuracies were compared to those achieved under SRS sampling. The chosen double-sampling estimators were favoured for several reasons: **(i)** the design-based frame considerably relaxes requirements on the regression model which seemed appropriate facing severe quality restrictions in the LiDAR data; **(ii)** the estimators can consider *non-exhaustive*, i.e. non wall-to-wall, auxiliary information; **(iii)** all estimators are explicitly formulated for cluster sampling which has not yet been the case for frequently used model-dependent estimators; and **(iv)** the asymptotically unbiased g-weight variance accounts for the design-dependency of the regression coefficients on the sample (*in-*

1. INTRODUCTION

ternal model approach) and is also robust to heteroscedasticity of the model residuals.

The results from this study were considered to provide valuable information whether the suggested procedure a) might be a cost-saving alternative to a regional FDI and b) can be used as a reliable validation for SDI data. A secondary objective was to address the potential effects of auxiliary data quality on estimation precision, and to identify challenges when transferring the existing German NFI design into the suggested double sampling estimation procedure.

2 Terrestrial sampling design of the German NFI

The German National Forest Inventory (German NFI) is a periodic inventory that is carried out every 10 years over the entire forest area of Germany. The most recent inventory (BWI3) was conducted in the years 2011 and 2012. While information was originally gathered at a systematic 4x4 km grid, some federal states such as Rhineland-Palatinate have switched to a densified 2x2 km grid. The German NFI uses a cluster sampling design, which means that a sample unit consists of maximal four sample locations (also referred to as *sample plots*) that are arranged in a square (so called *cluster*) with a side length of 150 metres (Picture). The number of plots per cluster can however vary between 1 and 4 depending on forest/non-forest decisions by the field crews on the individual plot level ([Bundesministerium für Ernährung, 2011](#)). In the field survey of the BWI3, sample trees for timber volume estimation are selected according to the angle count sampling technique ([Bitterlich, 1984](#)), using a basal area factor (BAF) of 4 that is respectively adjusted for sample trees at the forest boundary by a geometric intersection of the boundary transect with the tree-individual inclusion circle ([Bundesministerium für Ernährung, 2011](#)). A further inventory threshold for a tree to be recorded is a diameter at breast height (dbh) of at least 7 cm. For each sample tree that is selected by this procedure, the dbh, the absolute tree height, the tree diameter at 7 m (D7) and the tree species is measured and used to calculate a volume estimation on the tree level. These volume estimations are based on the application of tree species specific taper curves that are adjusted to the set of diameters and corresponding height measurements taken from the respective sample tree ([Kublin et al, 2013](#)).

3 Double sampling in the infinite population approach

The estimators used in this study have been proposed by ([Mandallaz, 2013a; Mandallaz et al, 2013](#)) and build upon the so called infinite population approach (IPA) in order to bridge the inventory procedure and the derived information to the mathematics behind the estimators. Therefore, we shall first provide a short introduction into this general estimation frame. We start by assuming that the population P of trees $i \in 1, 2, \dots, N$ within a forest of interest F is exactly defined, and each tree i has a directly or indirectly observable response variable Y_i (e.g. its timber volume) that allows to specify the population mean Y (e.g., the average timber volume per unit area) over F . If a full census of all tree population individuals is not possible, Y has to be estimated by the conduction of an inventory. The infinite population approach assumes that the spatial distribution of the local density $Y(x)$ (e.g., the timber volume per unit area) at each point or location x in the forest F is given by a fixed (i.e. non stochastic) piecewise constant function. The population mean Y is thus mathematically equivalent to the integral of the density function surface divided by the forest area $\lambda(F)$, i.e. $Y = \frac{1}{\lambda(F)} \sum_{i=1}^N Y_i = \frac{1}{\lambda(F)} \int_F Y(x) dx$, and thus the population mean Y corresponds to a spatial mean. Since the local density function is in practice always unknown, one estimates Y by collecting a sample s_2 of all local density values by the conduction of a terrestrial inventory at n_2 uniformly and independently

distributed sample points over F . This procedure is often referred to as *one-phase sampling* (OPS). Opposed to the one-phase approach, *two-phase* or *double-sampling* procedures use information from two nested samples (phases). Practically speaking, the terrestrial inventory s_2 is embedded in a large phase s_1 comprising n_1 sample locations that each provide a set of explanatory variables described by the column vector $\mathbf{Z}(x) = (z(x)_1, z(x)_2, \dots, z(x)_p)^\top$ at each point $x \in s_1$. These explanatory variables are derived from auxiliary information that is available in high quantity within the forest F . For every $x \in s_1$, $\mathbf{Z}(x)$ is transformed into a prediction $\hat{Y}(x)$ of $Y(x)$ using the choice of some prediction model. The basic idea of this method is to boost the sample size by providing a large sample of less precise but cheaper predictions of $Y(x)$ in s_1 and to correct any possible model bias, i.e., $\mathbb{E}(Y(x) - \hat{Y}(x))$, using the subsample of terrestrial inventory units where the value of $Y(x)$ is observed.

4 Estimators

4.1 Design-based SRS estimator for cluster sampling

The simple random sampling (SRS) estimator for cluster sampling constitutes the *status quo* that is currently applied under the existing one-phase sampling design of the German NFI in order to obtain a point and variance estimate for the mean timber volume of a given estimation unit. In order to provide all estimators in the infinite population framework and ensure a consistent terminology with the two-phase estimators in Section 4.2, we will introduce the SRS estimator that is applied in the BWI3 algorithms ([Schmitz et al, 2008](#)) in the form given in [Mandallaz \(2008\)](#); [Mandallaz et al \(2016\)](#).

In order to calculate the local density $Y_c(x)$ at the cluster level, a cluster is defined as consisting of M sample locations (in the BWI3, we have $M = 4$) where $M - 1$ sample locations x_2, \dots, x_M are created close to the cluster origin x_1 by adding a fixed set of spatial vectors e_2, \dots, e_M to x_1 . The actual number of plots per cluster, $M(x)$, is a random variable due to the uniform distribution of x_l ($l = 1, \dots, M$) in the forest F and forest/non-forest decision for each sample location x_l :

$$M(x) = \sum_{l=1}^M I_F(x_l) \quad \text{where} \quad I_F(x_l) = \begin{cases} 1 & \text{if } x_l \in F \\ 0 & \text{if } x_l \notin F \end{cases} \quad (1)$$

The local density on cluster level $Y_c(x)$, in our case the timber volume per hectare, is then defined as the average of the individual sample plot densities $Y(x_l)$:

$$Y_c(x) = \frac{\sum_{l=1}^M I_F(x_l) Y(x_l)}{M(x)} \quad (2)$$

The local density $Y(x_l)$ on individual sample plot level was calculated according to the description in [Mandallaz \(2008\)](#), which can be rewritten for angle-count sampling technique

applied in the BWI3. The general form of $Y(x)$ in [Mandallaz \(2008\)](#) is given as the Horwitz-Thompson estimator

$$Y(x_l) = \sum_{i \in s_2(x_l)} \frac{Y_i}{\pi_i \lambda(F)} \quad (3)$$

where Y_i is in our case the predicted timber volume of the tree i recorded at sample location x in m^3 . Each tree has an inclusion probability π_i that is well defined as the proportion of its inclusion circle area $\lambda(K_i)$ within the forest area $\lambda(F)$, i.e. via their geometric intersection:

$$\pi_i = \frac{\lambda(K_i \cap F)}{\lambda(F)} \quad (4)$$

The radius R_i of the tree-individual inclusion circle K_i is given by $R_i = bhd_i/cf_{i,corr}$ (also referred to as *limiting distance*), where $cf_{i,corr}$ is the counting factor corrected for potential boundary effects at the forest border. In case of angle-count sampling, we can rewrite π_i as

$$\pi_i = \frac{G_i}{cf_{i,corr}\lambda(F)} \quad (5)$$

since the intersection area $\lambda(K_i \cap F)/\lambda(F)$ can be expressed using the trees basal area G_i (in m^2) and the corrected counting factor:

$$\lambda(K_i \cap F) = \frac{G_i}{cf_{i,corr}} \quad \text{where} \quad cf_{i,corr} = cf \frac{\lambda(K_i)}{\lambda(K_i \cap F)} \quad (6)$$

Using Eq. 5 in Eq. 3 yields the rewritten form of $Y(x_l)$ for angle count sampling that conforms to the definition used in the BWI3 algorithms ([Schmitz et al, 2008](#)):

$$Y(x_l) = \sum_{i \in s_2(x_l)} \frac{cf_{i,corr}Y_i}{G_i} = \sum_{i \in s_2(x_l)} nha_i Y_i \quad (7)$$

where nha_i is the number of trees per hectare represented by tree i . The local densities on cluster level can then be used to derive the estimated spatial mean \hat{Y}_c and its estimated variance $\hat{\mathbb{V}}(\hat{Y}_c)$ for any given spatial unit for which $n_2 \geq 2$ (n_2 denoting the number of sample units, i.e. clusters):

$$\hat{Y}_c = \frac{\sum_{x \in s_2} M(x) Y_c(x)}{\sum_{x \in s_2} M(x)} \quad (8a)$$

$$\hat{\mathbb{V}}(\hat{Y}_c) = \frac{1}{n_2(n_2 - 1)} \sum_{x \in s_2} \left(\frac{M(x)}{\bar{M}_2} \right)^2 (Y_c(x) - \hat{Y}_c)^2 \quad (8b)$$

4.2 Design-based small area regression estimators for cluster sampling

All three considered small area estimators have in common that they use ordinary least square (OLS) regression models to produce the predictions of the local density $Y_c(x)$ directly on the cluster level c . We consider the *internal model approach*, where the vector of estimated regression coefficients on the cluster level is found by "borrowing strength" from the entire terrestrial sample s_2 of the current inventory:

$$\hat{\boldsymbol{\beta}}_{c,s_2} = \mathbf{A}_{c,s_2}^{-1} \left(\frac{1}{n_2} \sum_{x \in s_2} M(x) Y_c(x) \mathbf{Z}_c(x) \right) \quad (9a)$$

$$\mathbf{A}_{c,s_2} = \frac{1}{n_2} \sum_{x \in s_2} M(x) \mathbf{Z}_c(x) \mathbf{Z}_c^\top(x) \quad (9b)$$

$\mathbf{Z}_c(x)$ is the vector of explanatory variables on the cluster level, which is calculated as the weighted average of the explanatory variables $\mathbf{Z}(x_l)$ on the individual plot levels x_1, \dots, x_l (Eq.10). The weight $w(x_l)$ is the proportion of the support-area within the forest F used to derive the explanatory variables from the raw auxiliary information.

$$\mathbf{Z}_c(x) = \frac{\sum_{l=1}^M I_F(x_l) w(x_l) \mathbf{Z}(x_l)}{\sum_{l=1}^M I_F(x_l) w(x_l)} \quad (10)$$

The estimated design-based variance-covariance matrix $\hat{\Sigma}_{\hat{\boldsymbol{\beta}}_{s_2}}$ accounts for the fact that the regression model is internal by reflecting the dependency of the estimated regression coefficients on the realized sample s_2 . It is defined as

$$\hat{\Sigma}_{\hat{\boldsymbol{\beta}}_{s_2}} = \mathbf{A}_{c,s_2}^{-1} \left(\frac{1}{n_2^2} \sum_{x \in s_2} M^2(x) \hat{R}_c^2(x) \mathbf{Z}_c(x) \mathbf{Z}_c^\top(x) \right) \mathbf{A}_{c,s_2}^{-1} \quad (11)$$

with $\hat{R}_c = Y_c(x) - \mathbf{Z}_c^\top(x) \hat{\boldsymbol{\beta}}_{c,s_2}$ being the empirical model residuals at the cluster level, which by construction of OLS satisfy the important *zero mean residual property*, i.e. $\frac{\sum_{x \in s_2} M(x) \hat{R}_c(x)}{\sum_{x \in s_2} M(x)} = 0$.

In the following, we will give a short description of each small area estimator and refer to [Mandalaz \(2013a\)](#); [Mandalaz et al \(2016, 2013\)](#) if the reader requires additional details or proofs. The estimators have also been implemented in the R-package *forestinventory* ([Hill and Massey, 2017](#)) which was used to compute all estimates in this study.

4.2.1 Pseudo Small Area Estimator (PSMALL)

All point information used for small area estimation is now restricted to that available at the sample locations $s_{1,G}$ or $s_{2,G}$ in the small area G , with exception of $\hat{\boldsymbol{\beta}}_{c,s_2}$ and $\hat{\Sigma}_{\hat{\boldsymbol{\beta}}_{c,s_2}}$ which are

always based on the entire sample s_2 . We thus first define the following quantities on the small area level:

$$\hat{\mathbf{Z}}_{c,G} = \frac{\sum_{x \in s_{1,G}} M_G(x) \mathbf{Z}_{c,G}(x)}{\sum_{x \in s_{1,G}} M_G(x)} \quad \text{where } \mathbf{Z}_{c,G}(x) = \frac{\sum_{l=1}^L I_G(x_l) \mathbf{Z}(x_l)}{M_G(x)} \quad (12a)$$

$$Y_{c,G}(x) = \frac{\sum_{l=1}^L I_G(x_l) \mathbf{Y}(x_l)}{M_G(x)} \quad \text{and } \hat{Y}_{c,G}(x) = \hat{\mathbf{Z}}_{c,G}^\top \hat{\boldsymbol{\beta}}_{c,s_2} \quad (12b)$$

$$\bar{R}_{2,G} = \frac{\sum_{x \in s_{2,G}} M_G(x) \hat{R}_{c,G}(x)}{\sum_{x \in s_{2,G}} M_G(x)} \quad \text{where } \hat{R}_{c,G}(x) = Y_{c,G}(x) - \hat{Y}_{c,G}(x) \quad (12c)$$

Note that the restriction to G , i.e. $I_G(x_l) = \{0, 1\}$, is made on the individual sample plot level x_l , and $M_G(x) = \sum_{l=1}^L I_G(x_l)$ thus is the number of sample plots per cluster within the small area. The asymptotically design-unbiased point estimate of *PSMALL* is then defined according to Eq. 13a. The first term estimates the small area population mean of G by applying the globally derived regression coefficients to the small area cluster means of the explanatory variables $\hat{\mathbf{Z}}_{c,G}$. The second term then corrects for a potential bias of the regression model predictions in the small area G by adding the mean of the empirical residuals $\bar{R}_{2,G}$ in G . This correction insures that the *zero mean residual property* in F also holds within the small area G , which is per se not ensured by fitting the regression coefficients with data outside G .

$$\hat{Y}_{c,G,PSMALL} = \hat{\mathbf{Z}}_{c,G}^\top \hat{\boldsymbol{\beta}}_{c,s_2} + \bar{R}_{2,G} \quad (13a)$$

$$\begin{aligned} \hat{\mathbb{V}}(\hat{Y}_{c,G,PSMALL}) &= \hat{\mathbf{Z}}_{c,G}^\top \hat{\boldsymbol{\Sigma}}_{\hat{\boldsymbol{\beta}}_{c,s_2}} \hat{\mathbf{Z}}_{c,G} + \hat{\boldsymbol{\beta}}_{c,s_2}^\top \hat{\boldsymbol{\Sigma}}_{\hat{\mathbf{Z}}_{c,G}} \hat{\boldsymbol{\beta}}_{c,s_2} \\ &\quad + \frac{1}{n_{2,G}(n_{2,G}-1)} \sum_{x \in s_{2,G}} \left(\frac{M_G(x)}{\bar{M}_{2,G}} \right)^2 (\hat{R}_{c,G}(x) - \bar{R}_{2,G})^2 \end{aligned} \quad (13b)$$

The estimated design-based variance of $\hat{Y}_{c,G,PSMALL}$ is given by Eq. 13b. Basically, the first term constitutes the variance introduced by the uncertainty in the regression coefficients, whereas the second term expresses the variance caused by estimating the exact auxiliary mean in G using a non-exhaustive sample $s_{1,G}$. The third term is the variance of the model residuals and thus accounts for the inaccuracies of the model predictions. Note that the first term can also be rewritten using g-weights (Mandalaz et al, 2016, pg.14) which ensure calibration properties of the auxiliary variables on the terrestrial sample.

The variance-covariance matrix of the auxiliary vector $\hat{\boldsymbol{\Sigma}}_{\hat{\mathbf{Z}}_{c,G}}$ is thereby defined as

$$\hat{\boldsymbol{\Sigma}}_{\hat{\mathbf{Z}}_{c,G}} = \frac{1}{n_{1,G}(n_{1,G}-1)} \sum_{i \in s_{1,G}} \left(\frac{M_G(x)}{\bar{M}_{1,G}} \right)^2 (\mathbf{Z}_{c,G}(x) - \hat{\mathbf{Z}}_{c,G})(\mathbf{Z}_{c,G}(x) - \hat{\mathbf{Z}}_{c,G})^\top \quad (14)$$

$$\text{with } \bar{M}_{1,G} = \frac{\sum_{i \in s_{1,G}} M_G(x)}{n_{1,G}}.$$

4.2.2 Pseudo Synthetic Estimator (PSYNTH)

The *PSYNTH* estimator is commonly applied when no terrestrial sample is available within the small area G (i.e. $n_{2,G} = 0$). The point estimate (Eq. 15a) is thus only based on the predictions generated by applying the globally derived regression coefficients to the small area cluster means of the explanatory variables $\hat{\mathbf{Z}}_{c,G}$. Note that the bias correction term using the empirical residuals (Eq. 13a) can no longer be applied. The *PSYNTH* estimator thus has a potential unobservable design-based bias.

$$\hat{Y}_{c,G,PSYNTH} = \hat{\mathbf{Z}}_{c,G}^\top \hat{\boldsymbol{\beta}}_{c,s_2} \quad (15a)$$

$$\hat{\mathbb{V}}(\hat{Y}_{c,G,PSYNTH}) = \hat{\mathbf{Z}}_{c,G}^\top \hat{\boldsymbol{\Sigma}}_{\hat{\boldsymbol{\beta}}_{c,s_2}} \hat{\mathbf{Z}}_{c,G} + \hat{\boldsymbol{\beta}}_{c,s_2}^\top \hat{\boldsymbol{\Sigma}}_{\hat{\mathbf{Z}}_{c,G}} \hat{\boldsymbol{\beta}}_{c,s_2} \quad (15b)$$

The uncertainty of the model predictions can also no longer be considered in the variance estimation (Eq. 15b). The synthetic estimator will therefore usually have a smaller variance than estimators incorporating the model uncertainties, but at the cost of a potential bias. Note that the *PSYNTH* estimator is still design-based, but one purely has to rely on the validity of the regression model within the small area as it is the case in the model-dependent framework.

4.2.3 Extended Pseudo Synthetic Estimator (EXTPSYNTH)

The *EXTPSYNTH* estimator (Eq. 16) has been proposed by [Mandallaz \(2013a\)](#) as a transformed version of the *PSMALL* estimator that has the form of the *PSYNTH* estimator but remains asymptotically design unbiased. It has the advantage that the mean of the empirical model residuals of the OLS regression model for the entire area F and the small area G are by construction both zero at the same time, i.e. $\bar{R}_c = \bar{R}_{c,G} = 0$. This is realized by *extending* the auxiliary vector $\mathbf{Z}_c(x)$ by the indicator variable $I_{c,G}$ which takes the value 1 if the entire cluster lies within the small area G and 0 if the entire cluster is outside G , i.e. $I_{c,G}(x) = \frac{M_G(x)}{M(x)}$. The extended auxiliary vector thus becomes $\mathbf{Z}_c^\top(x) = (\mathbf{Z}_c^\top(x), I_{c,G}(x))$ and the new regression coefficient using $\mathbf{Z}_c(x)$ instead of $\mathbf{Z}_c(x)$ in Eq. 9 is denoted as $\hat{\boldsymbol{\theta}}_{s_2}$. All remaining components are calculated by plugging in $\mathbf{Z}_c(x)$ in Eq. 12. A decomposition of $\hat{\boldsymbol{\theta}}_{s_2}$ reveals that the residual correction term is now included in the regression coefficient $\hat{\boldsymbol{\theta}}_{s_2}$.

$$\hat{Y}_{c,G,EXTPSYNTH} = \hat{\mathbf{Z}}_{c,G}^\top \hat{\boldsymbol{\theta}}_{c,s_2} \quad (16a)$$

$$\hat{\mathbb{V}}(\hat{Y}_{c,G,EXTPSYNTH}) = \hat{\mathbf{Z}}_{c,G}^\top \hat{\boldsymbol{\Sigma}}_{\hat{\boldsymbol{\theta}}_{c,s_2}} \hat{\mathbf{Z}}_{c,G} + \hat{\boldsymbol{\theta}}_{c,s_2}^\top \hat{\boldsymbol{\Sigma}}_{\hat{\mathbf{Z}}_{c,G}} \hat{\boldsymbol{\theta}}_{c,s_2} \quad (16b)$$

However, it is important to note that $\bar{R}_{c,G} = 0$ under the extended regression model only holds if the sample plots x_1, \dots, x_l of a cluster are *all* either inside or outside the small area, i.e. $M_G(x) \equiv M(x)$, and thus $I_{c,G}(x) = \frac{M_G(x)}{M(x)}$ can only take the values 1 or 0. [Mandallaz](#)

et al (2016) assumed that the effects on the estimates should be negligible as the number of occasions where $M_G(x) < M(x)$ was considered to be small in practical implementations. It was thus a further objective of this study to investigate the actual occurrences and effects of this phenomenon by comparing the estimates of *EXTPSYNTH* to those of *PSMALL*.

4.3 Measures of estimation accuracy

The estimation accuracies were quantified by the *estimation error*, which is the ratio of the standard error and the point estimate:

$$error(\hat{Y})_{[\%]} = \frac{\sqrt{\hat{V}(\hat{Y})}}{\hat{Y}} * 100 \quad (17)$$

We further calculated the 95% confidence interval for each estimate for visualization purpose. The confidence intervals can also be used for hypothesis testing whether the point estimates of the three estimators for a given small area are statistically different. The confidence intervals under SRS can be obtained as:

$$CI_{1-\alpha}(\hat{Y}) = \left[\hat{Y} - t_{n_2-1,1-\frac{\alpha}{2}} \sqrt{\hat{V}(\hat{Y})}, \hat{Y} + t_{n_2-1,1-\frac{\alpha}{2}} \sqrt{\hat{V}(\hat{Y})} \right] \quad (18)$$

The confidence intervals for the *PSMALL* and *EXTPSYNTH* estimates are calculated as:

$$CI_{1-\alpha}(\hat{Y}) = \left[\hat{Y} - t_{n_{2,G}-1,1-\frac{\alpha}{2}} \sqrt{\hat{V}(\hat{Y})}, \hat{Y} + t_{n_{2,G}-1,1-\frac{\alpha}{2}} \sqrt{\hat{V}(\hat{Y})} \right] \quad (19)$$

For the *PSYNTH* estimates, the confidence intervals are

$$CI_{1-\alpha}(\hat{Y}) = \left[\hat{Y} - t_{n_2-p,1-\frac{\alpha}{2}} \sqrt{\hat{V}(\hat{Y})}, \hat{Y} + t_{n_2-p,1-\frac{\alpha}{2}} \sqrt{\hat{V}(\hat{Y})} \right] \quad (20)$$

In order to address the potential benefits of the small area estimators compared with the SRS approach, we calculated the *relative efficiency* (Eq. 21) which can be interpreted as the relative sample size under SRS needed to achieve the variance under the double sampling estimators.

$$rel.eff = \frac{\hat{V}_{SRS}(\hat{Y})}{\hat{V}_{SAE_{2phase}}(\hat{Y})} \quad (21)$$

5 Case study

5.1 Study area and small area units

The German federal state Rhineland-Palatinate (*RLP*) is located in the western part of Germany and borders Luxembourg, France and Belgium. With 42.3% (appr. 8400 km²) of the entire state area (19850 km²) covered by forest, RLP is one of the two states with the highest forest coverage among all federal states of Germany ([Thünen-Institut, 2014](#)). The forests of RLP are further characterized by a pronounced diversity in bioclimatic growing conditions that have strong influence on the local growth dynamics as well as tree species composition ([Gauer and Aldinger, 2005](#)) and are further characterized by large variety of forest structures ranging from characteristic oak coppices (Moselle valley), pure spruce, beech and scots pine forests (i.a. Hunsrück and Palatinate forest) up to mixed forests comprising variable proportions of oak, larch, spruce, Scots pine and beech. Around 82% of the forest area in RLP are mixed forest stands and 69% of the forest area exhibit a multi-layered vertical structure. The forest area of RLP are divided into 3 ownership classes, i.e. state forest (27%), communal forest (46%) and privately owned forest (27%). The forest service of RLP has the legal mandate to sustainably manage the state and communal forest area (73% of the entire forest area), including forest planning, harvesting and the sale of wood ([LWaldG, 2000](#)). For this reason, the entire forest area has been spatially organised in 3 main hierarchical management units (Figure 1). On the upper level, RLP has been divided into 45 Forstämter (*FA*), which are further divided into a total number of 405 Forstreviere (*FR*). The next level are the forest stands (104'184 in total) for which expert judgements are conducted by SFIs in a 5- to 10 year period in order to set up management strategies for the upcoming 10 years. The FAs and FRs constituted the small area (*SA*) units for which design-based small area estimations of the mean standing timber volume were calculated by incorporating the available terrestrial inventory data of the BWI3 in the estimators described in Section 4. The average area of the SA units were 43'777 ha on the FA-level, and 4624 ha on the FR level.

5.2 Terrestrial sample

Rhineland-Palatinate (*RLP*) is covered by a 2x2 km inventory grid of the German NFI. In the last inventory (BWI3) conducted in the year 2013, timber volume information was derived for 2810 cluster (8092 plots) in the field survey. The local timber volume density on the plot and cluster level for this sample was consequently calculated according to Section 4.1. In the frame of this survey, the plot center coordinates were re-measured with differential global satellite navigation system (DGPS) technique. Knowledge about the exact plot positions were considered crucial to provide optimal comparability between the terrestrially observations and the information derived from the auxiliary information. A comparison of the DGPS coordinates with the so-far used target coordinates revealed that 90% of all horizontal deviations lay in the range of 25 meters. A detailed analysis of horizontal DGPS errors in

5. CASE STUDY

RLP by [Lamprecht et al \(2017\)](#) indicated that 80% of the plots should not exceed horizontal DGPS errors of 8 meters. For 162 plots, the DGPS coordinates were replaced by their target coordinates due to missingness or implausible values. The terrestrial sample size $n_{2,G}$ within the FA units was 46 cluster on average and ranged between 11 and 64. Within the FR units, $n_{2,G}$ was considerably smaller with an average of 5 cluster and a range between 0 and 13.

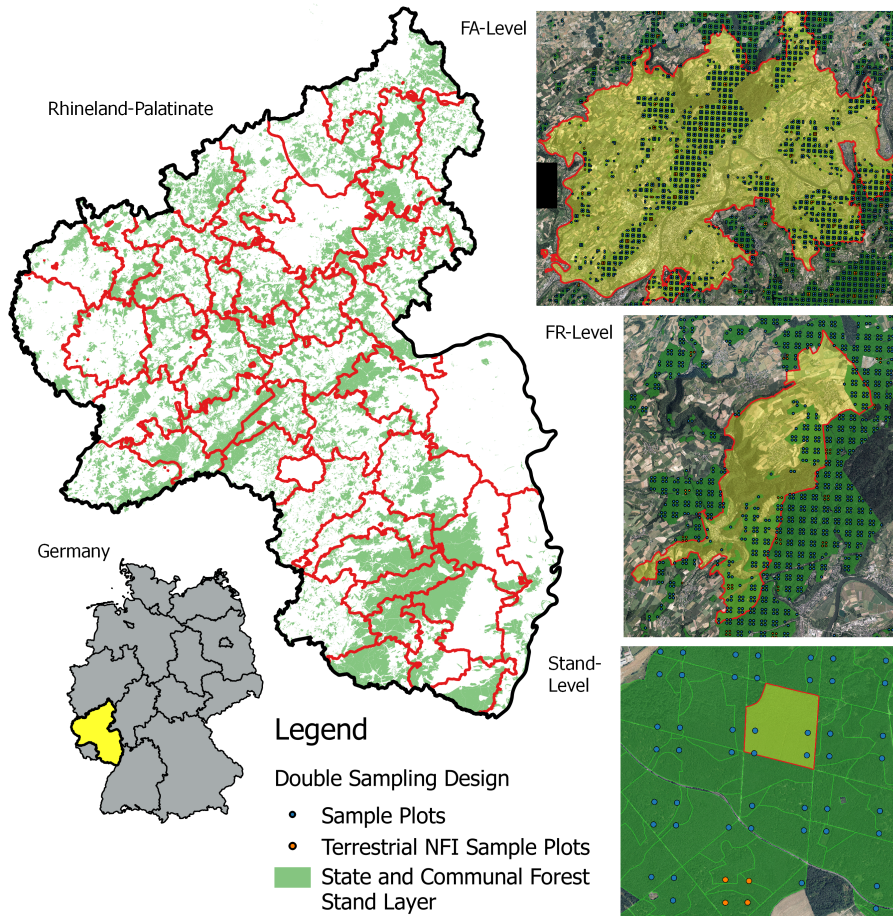


Figure 1: *Left:* Study Area with delineated FA forest management units. *Right:* Example for each of the three management units (from top to bottom): FA, FR and forest stand unit with overlayed the extended double sampling cluster design. *Green:* Forest stand polygon layer defining the forest area of this study.

5.3 Extension to double sampling design

In order to apply the small area estimators (Section [\(4.2\)](#)), the existing NFI design was extended to a double sampling design by densifying the existing systematic 2x2 kilometer grid to a grid size of 500x500 meters that constituted the large first phase s_1 in accordance to Section [3](#) (Figure [1, right](#)). The existing terrestrial phase s_2 was consequently integrated by

replacing the target coordinates of the respective s_1 cluster by the terrestrially measured DGPS coordinates. For our study, we restricted the *sampling frame* to the communal and state forest. The forest/non-forest decision for each plot was thereby made by a spatial intersection of the plot center coordinates with a polygon layer of the communal and state forest stands provided by the forest service. Using this stand layer provided the advantage to consistently apply the same forest/non-forest definition to the entire sample s_1 in order to decide about excluding or including a plot in the sampling frame. The terrestrial sample size n_2 was thus reduced to 2055 cluster (5791 plots). Table 1 provides a short descriptive summary about the volume densities and the main attributes of the NFI plots located in the state and communal forest sampling frame. The densification led to an average sample size $n_{1,G}$ of 759 cluster (range: 246 – 1022) in the FA units, and 88 cluster (range: 1 – 194) in the FR units.

Table 1: Descriptive statistics of the forest observed on NFI sample plots located within communal and state forest area (n=5791).

Variable	Mean	SD	Maximum
Timber Volume (m ³ /ha)	300.86	195.55	1375.31
Mean DBH (mm)	354.90	137.22	1123.20
Mean height (dm)	239.60	72.43	497.43
Mean stem density per hectare	101.00	114.01	1010.31

5.4 Auxiliary information

5.4.1 LiDAR canopy height model

A prerequisite for the application of the suggested two-phase small area estimators was the identification of suitable auxiliary information that is available over the entire study area. Between the year 2003 and 2013, the topographic survey institution of RLP conducted an air-borne laser scanning (LiDAR) acquisition over the entire federal state at leaf-off condition in order to derive a countrywide digital terrain and surface model. For this study, the recorded LiDAR data was used to create a canopy height model (CHM) in raster format, providing discrete information about the canopy surface height of the forest area in a spatial resolution of 5 meters (Figure 2, *top*). The CHM was calculated as the difference between the digital terrain model (DTM) and the digital surface model (DSM) that were derived by a Delauney interpolation of the two separated LiDAR point clouds (ground pulses and first pulses from non-ground objects). Based on numerous studies (e.g. [Maack et al \(2016\)](#)), the CHM was considered to provide the most valuable information to be used in the OLS regression model for predicting the timber volume on sample plot level. However, during the extended acquisition period, airborne laser scanning technology evolved significantly, which lead to severe quality variations in the CHM. In particular, the LiDAR acquisition recorded in 2002 and 2003 exhibited a rather poor quality with about only 1 point per 5x5 m², while more recently acquired datasets contained more than 125 points per 5x5 m² raster cell. Furthermore, due to sensor

failures, CHM information was not available at 16 sample locations (none of them considered terrestrial sample plots of the s_2 phase though). These plots were deleted from the sampling frame and its non-available information thus treated as missing at random. This assumption was considered to be reasonable as the respective sample locations did not exclude specific forest structures.

5.4.2 Tree species map

The second source of auxiliary information was a countrywide satellite-based classification map of the five main tree species (European beech, Sessile and Pedunculate oak, Norway spruce, Douglas fir, Scots pine) described in [Stoffels et al \(2015\)](#) (Figure 2, *bottom*). The classified tree species map has a grid size of 5 meters and was calculated from 22 bi-temporal satellite images (SPOT5 and RapidEye) by application of a spatially adaptive classification algorithm described in [Stoffels et al \(2012\)](#). As timber volume estimations on the tree level are often based on species-specific biomass and volume equations, the use of tree species information - especially for timber volume estimation - has often been stated as a key factor for improving the estimation precision [White et al \(2016\)](#). In this respect, incorporating the tree species map information was particularly attractive as it predicts five of the seven tree species that are used in the BWI3 taper functions ([Kublin et al, 2013](#)) to calculate the timber volume of a sample tree. However, due to unavailable satellite data for the classification, the tree species map excluded one large patch with an area of 415 km² in the south-west part of RLP covering an entire FA-unit (10 FR units respectively). In 9 additional FR units, the tree species information was also missing for a subset of the sample locations due to two additional patches with an area of 76 km² and 100 km² in the northern part of RLP. For these parts, small area estimation was thus restricted to using only the available CHM information in the regression model. With respect to model fitting, the tree species information was missing for 407 (7%) of the 5791 sample locations. A summary of the sample sizes and missing auxiliary information is again provided in Table 2.

Table 2: Sample size for each phase in entire study area. $n_{\{1,2\},plots}$: number of plots. $n_{\{1,2\}}$: number of cluster

<i>Sampling frame</i>	$n_{1,plot}$	n_1	$n_{2,plot}$	n_2
communal and state forest	96'854	33'365	5791	2055
missing CHM	18	10	0	0
missing TSPEC	7060	3587	414	385
missing CHM and TSPEC	3	2	0	0
missing CHM or TSPEC	7075	3595	414	385

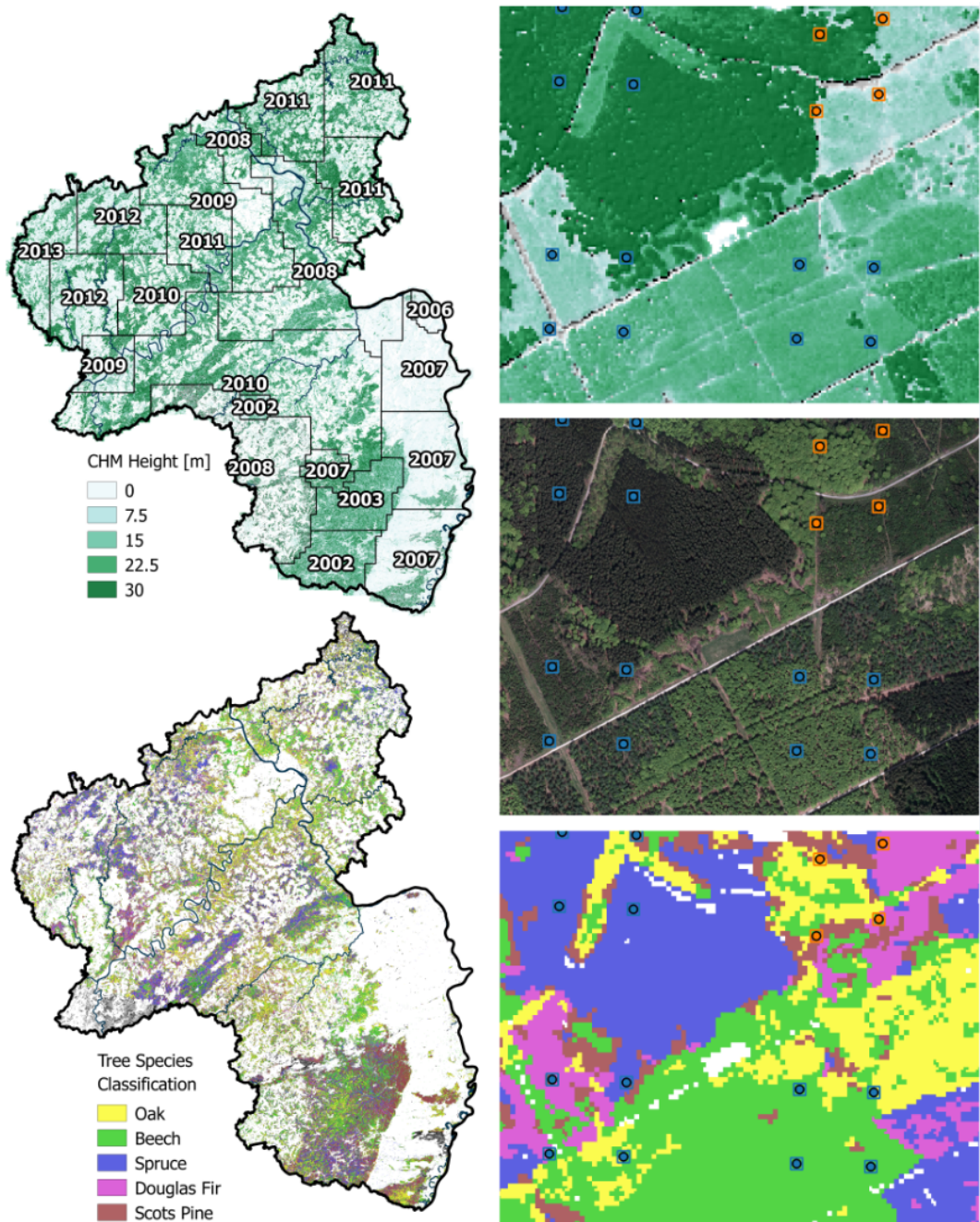


Figure 2: Left: CHM (top) and tree species classification map (bottom) available on the federal state level were used as auxiliary information. Right: Magnified illustration of the rectangular supports used to derive the explanatory variables from the auxiliary information.

5.5 Calculation of the auxiliary variables

5.5.1 LiDAR canopy height model

From the CHM, the mean canopy height (*meanheight*) and the standard deviation (*stddev*) was calculated by evaluating the raster values around each sample location within a predefined rectangular square (support) with a side length of 12 meters that was centered around the sample plot centers. Each support was previously intersected with the forest polygon layer in order to evaluate auxiliary information only within the forest definition. The percentage of the non-intersected support within the forest layer was used as the weight $w(x_l)$ introduced in Eq. 10. Furthermore, the year of the LiDAR acquisition (*lidaryear*) was derived as an additional categorical variable to account for the time-lag between the CHM information and the terrestrial survey as well as to explain heterogeneity in the data introduced by the varying LiDAR quality. Adjustments were made to the original acquisition years by introducing an additional factor level *2008_I* for a subset of the 2008 acquisition where the quality turned out to be considerably poor due to a sensor error. In addition, the years 2006 and 2007 as well as 2012 and 2013 were pooled in order to increase the number of observations per factor level, resulting in nine categories in total (2002, 2003, 2007, *2008_I*, 2008, 2009, 2010, 2011 and 2012).

5.5.2 Tree species map

The tree species map information was used to predict the main tree species of a sample plot (*treespecies*). This implied two consecutive processing steps. In the *first* step, one of the five tree species was assigned to a sample location if 100% of the raster values within the same support as used for the CHM were classified as that species. Otherwise, the sample location was assigned the value 'mixed'. It should be mentioned that the support size and the percentage threshold are parameters that can be optimised in order to achieve the best variance decomposition and thus improvement in model accuracy when using the categorical *treespecies* variable in a regression model. [Hill et al \(2018\)](#) conducted a detailed analysis of how to optimally derive the auxiliary variables for the present data set and identified the above described settings as the most suitable. It was additionally shown that using the random forest algorithm by [Breiman \(2001\)](#) for a calibration of the predicted main plot species on the actual main taper-function species derived from the terrestrial inventory data could boost the classification accuracy in the classes *Scots pine* and *Douglas Fir*, which performed considerably worse than the remaining species (Table 3). The calibration was able to considerably mitigate the effects of misclassification on the regression coefficients and thus allowed for an increase in model accuracy. In a *second* step, we thus provided the random forest algorithm in the statistical software R ([R Core Team, 2017](#)) with the actual main taper-function species derived from the terrestrial inventory data as response variable as well as a full set of p predictor variables that comprised the initial prediction of the main plot tree species (*treespecies*), the mean canopy height (*meanheight*) and standard deviation (*stddev*) derived from the CHM, the proportion of coniferous trees estimated from the tree species classification map (*prop.conif*)

and the bioclimatic growing region (wgb) at the sample location. The algorithm was grown with 2000 trees, considering $\sqrt{p} \approx 3$ of the predictors for each split. The resulting random forest model was consequently applied at all sample locations s_1 to provide the *treespecies* variable.

Table 3: Classification accuracies of the *treespecies* variable before and after calibration. n_{ref} : number of terrestrial reference plots. n_{class} : number of classified plots.

Main plot species	Producer's accuracy[%]		User's accuracy[%]		nref	nclass	
	uncalib	calib	uncalib	calib		uncalib	calib
Beech	29.56	22.31	46.11	47.02	883	566	419
Douglas Fir	33.04	24.78	47.50	48.72	230	160	117
Oak	47.75	11.07	24.34	48.48	289	567	66
Spruce	43.63	53.15	60.81	61.13	651	467	566
Scots Pine	55.87	22.91	29.59	46.07	179	338	89
Mixed	66.40	84.49	63.69	64.53	3152	3286	4127
Overall accuracy: 54.83% (61.96%)					5384	5384	

5.6 Regression Model

5.6.1 Design-Based Model Inference

6 Results

6.1 General estimation results

On FA level,

6.2 Estimation errors

On both small area levels, the design-unbiased estimators *PSMALL* and *EXTPSYNTH* led to a substantial reduction in the estimation errors compared to the SRS estimator (fig. 3). On the FA level, the SRS estimator yielded an estimation error of 6.7% on average compared to 5.2% and 4.8% under the *EXTPSYNTH* and *PSMALL* estimator. The cumulative error distribution (fig. 3, left) reveals that under the SRS estimator, errors $\leq 5\%$ were achieved for 17% of the FA units (8 of 45). This proportion could be increased to 62% (28 FA units) and 73% (33 FA units) by application of *PSMALL* and *EXTPSYNTH*. 95% of all estimates exhibited errors $\leq 9.5\%$ under the SRS estimator and $\leq 6.6\%$ when using *PSMALL* or *EXTPSYNTH*. Estimation errors higher than 10% only appeared twice for each of the unbiased estimators.

The error reduction by the unbiased double sampling estimators was even more pronounced on the FR level (fig. 3, right), although the overall error niveau was substantially higher than on FA level. The average error under the SRS estimator was 18.3%, while it was 11.3% and 12.2% under the *PSMALL* and *EXTPSYNTH* estimator. 95% of the 321 FR units where *PSMALL* and *EXTPSYNTH* could be applied exhibited errors $\leq 20\%$. In comparion, the SRS estimates resulted in errors $\leq 36.6\%$ for 95% of the 388 FR units and exceeded an error of 20% in 30% of the cases.

On both small area levels, the *PSYNTH* estimator resulted in much smaller estimation errors compared to *PSMALL* and *EXTPSYNTH*. This was as expected, since the *PSYNTH* variance estimate does not take the residual variation in each small area unit into account (section 4.2.2). Compared to the error distribution of the asymptotically design-unbiased estimators *PSMALL* and *EXTPSYNTH*, the estimation errors of *PSYNTH* might thus be to optimistic.

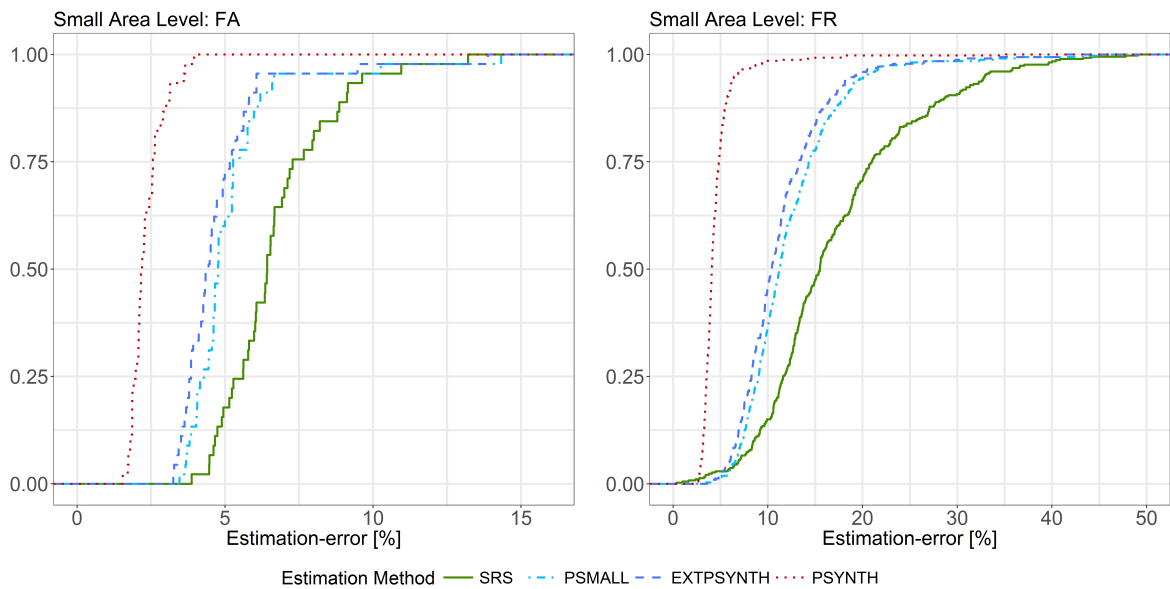


Figure 3: Cumulative distribution of estimation errors under the simple random sampling (SRS), the pseudo small (*PSMALL*), the extended pseudo synthetic (*EXTPSYNTH*) and the pseudo synthetic (*PSYNTH*) estimator. *Left:* Results for the 45 FA units. *Right:* Results for the 388 (SRS), 321 (*PSMALL* / *EXTPSYNTH*) and 403 (*PSYNTH*) FR units.

6.3 Comparison of PSMALL and EXTPSYNTH

As obvious from figure 3, the error distribution of *PSMALL* and *EXTPSYNTH* were found to be very similar, with *PSMALL* showing marginally higher estimation errors. In order to investigate the differences between *PSMALL* and *EXTPSYNTH*, we compared the g-weight variances of both estimators for all 321 FR units (fig. 4, left). As obvious, *PSMALL* yielded slightly larger variances for the vast majority of the estimates. As addressed in section 4.2.3, one possible explanation for such differences was the effect of one or more cluster not entirely being included in a small area unit, as this would constitute a violation of the *EXTPSYNTH* estimator. This violation was actually observed in 155 of the 321 FR units (48%). However, the affected FR units (depicted in red color, fig. 4) did not show a significant divergence from the *PSMALL* variances with respect to the remaining unaffected FR units. The variance differences between the two estimators were expected to occur for the following reason: as depicted in Mandallaz et al (2016, pp.17–18), the mathematical formulations of the *PSMALL* and *EXTPSYNTH* estimator are asymptotically equivalent only under large terrestrial sample sizes $n_{2,G}$ within the small area. An additional comparison of the absolute differences in the g-weight variance (fig. 4, right) revealed that large differences did in fact particularly occur for small area units with small terrestrial sample sizes ($n_{2,G} \leq 5$). The differences decreased with increasing sample size and thus confirmed the asymptotic relationship between the two estimators. However, a comparison of the confidence intervals of *PSMALL* and *EXTPSYNTH* revealed that the variance differences did not lead to statistically significant point estimates.

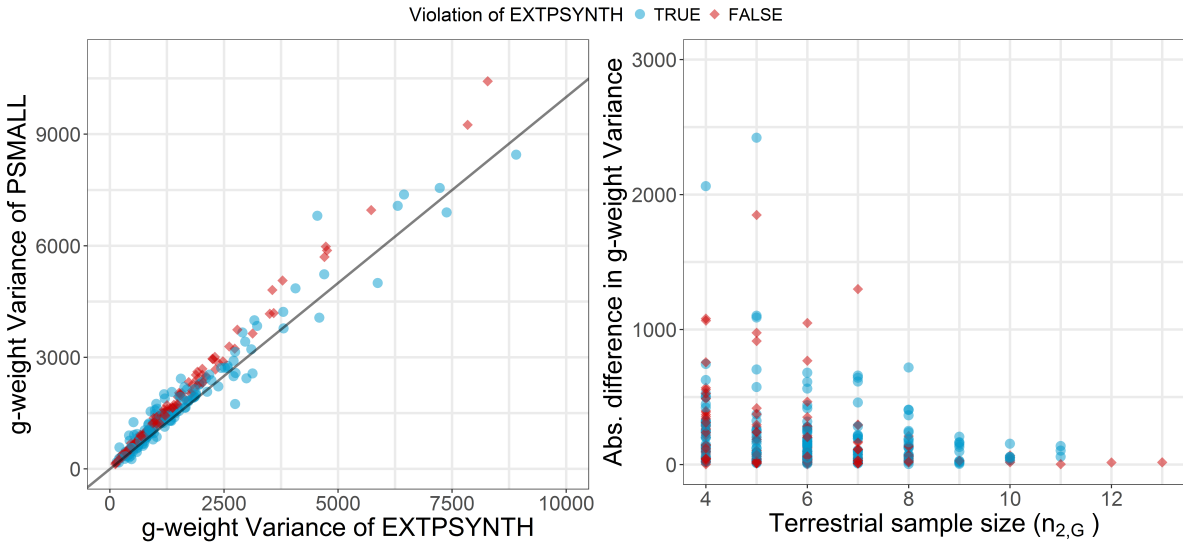


Figure 4: *Left:* Comparison of the g-weight variance between the PSMALL and the EXTPSYNTH estimator for the 321 FR units. *Right:* Difference in g-weight variance between the PSMALL and the EXTPSYNTH estimator in dependence of the terrestrial data (n_{2G}) in the FR unit.

6. RESULTS

6.4 Reduction of variance by two-phase estimators

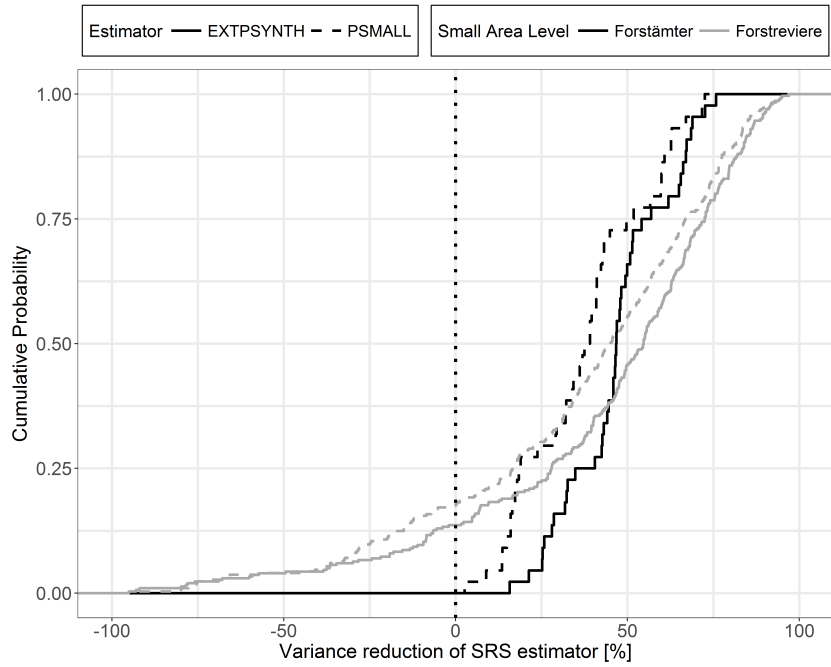


Figure 5: Cumulative distribution of variance reduction by the PSMALL and EXTPSYNTH compared to the SRS estimator for the 45 FA and 321 FR units.

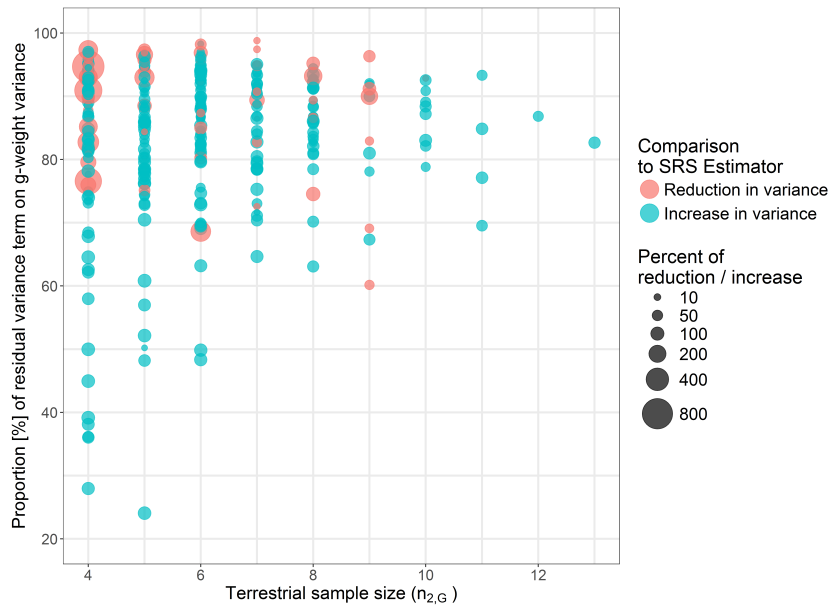


Figure 6

References

- Bitterlich W (1984) The relascope idea. Relative measurements in forestry. Commonwealth Agricultural Bureaux
- Böckmann T, Saborowski J, Dahm S, Nagel J, Spellmann H (1998) A new conception for forest inventory in lower saxony. *Forst und Holz* (Germany)
- Breidenbach J, Astrup R (2012) Small area estimation of forest attributes in the norwegian national forest inventory. *European Journal of Forest Research* 131(4):1255–1267, DOI 10.1007/s10342-012-0596-7
- Breiman L (2001) Random forests. *Machine learning* 45(1):5–32, DOI 10.1023/A:1010933404324
- Bundesministerium für Ernährung LuV (2011) Aufnahmeanweisung für die dritte Bundeswaldinventur BWI3 (2011 - 2012). URL <https://www.bundeswaldinventur.de/index.php?id=421>
- Gauer J, Aldinger E (2005) Waldökologische naturräume deutschlands-wuchsgebiete. *Mitteilungen des Vereins für Forstliche Standortskunde und Forstpflanzenzüchtung* 43:281–288
- Goerndt ME, Monleon VJ, Temesgen H (2011) A comparison of small-area estimation techniques to estimate selected stand attributes using lidar-derived auxiliary variables. *Canadian journal of forest research* 41(6):1189–1201
- Grafström A, Schnell S, Saarela S, Hubbell S, Condit R (2017) The continuous population approach to forest inventories and use of information in the design. *Environmetrics*
- Gregoire TG, Valentine HT (2007) Sampling strategies for natural resources and the environment. CRC Press
- Hill A, Massey A (2017) forestinventory: Design-Based Global and Small-Area Estimations for Multiphase Forest Inventories. R package version 0.3.1. URL <https://cran.r-project.org/web/packages/forestinventory/index.html>
- Hill A, Buddenbaum H, Mandallaz D (2018) Combining canopy height and tree species map information for large scale timber volume estimations under strong heterogeneity of auxiliary data and variable sample plot sizes, submitted for publication
- Koch B (2010) Status and future of laser scanning, synthetic aperture radar and hyperspectral remote sensing data for forest biomass assessment. *ISPRS Journal of Photogrammetry and Remote Sensing* 65(6):581–590, DOI 10.1016/j.isprsjprs.2010.09.001, URL <https://doi.org/10.1016/j.isprsjprs.2010.09.001>
- Köhl M, Magnussen SS, Marchetti M (2006) Sampling methods, remote sensing and GIS multiresource forest inventory. Springer Science & Business Media

- Kublin E, Breidenbach J, Kändler G (2013) A flexible stem taper and volume prediction method based on mixed-effects b-spline regression. European journal of forest research 132(5-6):983–997, DOI 10.1007/s10342-013-0715-0
- Kuliešis A, Tomter SM, Vidal C, Lanz A (2016) Estimates of stem wood increments in forest resources: comparison of different approaches in forest inventory: consequences for international reporting: case studyof european forests. Annals of Forest Science 73(4):857–869
- Lamprecht S, Hill A, Stoffels J, Udelhoven T (2017) A machine learning method for co-registration and individual tree matching of forest inventory and airborne laser scanning data. Remote Sensing 9(5), DOI 10.3390/rs9050505, URL <http://www.mdpi.com/2072-4292/9/5/505>
- von Lüpke N (2013) Approaches for the optimisation of double sampling for stratification in repeated forest inventories. PhD thesis, University of Göttingen
- von Lüpke N, Hansen J, Saborowski J (2012) A three-phase sampling procedure for continuous forest inventory with partial re-measurement and updating of terrestrial sample plots. European Journal of Forest Research 131(6):1979–1990, DOI 10.1007/s10342-012-0648-z
- LWaldG (2000) Landeswaldgesetz Rheinland-Pfalz (Forest Act Rhineland-Palatinate). URL <http://www.landesrecht.rlp.de>, Rhineland-Palatinate, Germany
- Maack J, Lingenfelder M, Weinacker H, Koch B (2016) Modelling the standing timber volume of baden-württemberg—a large-scale approach using a fusion of landsat, airborne lidar and national forest inventory data. International Journal of Applied Earth Observation and Geoinformation 49:107–116, DOI 10.1016/j.jag.2016.02.004, URL <https://doi.org/10.1016/j.jag.2016.02.004>
- Magnussen S, Mandallaz D, Breidenbach J, Lanz A, Ginzler C (2014) National forest inventories in the service of small area estimation of stem volume. Canadian Journal of Forest Research 44(9):1079–1090
- Magnussen S, Mauro F, Breidenbach J, Lanz A, Kändler G (2017) Area-level analysis of forest inventory variables. European Journal of Forest Research pp 1–17
- Mandallaz D (2008) Sampling techniques for forest inventories. CRC Press, DOI 10.1201/9781584889779, URL <https://doi.org/10.1201/9781584889779>
- Mandallaz D (2013a) Design-based properties of some small-area estimators in forest inventory with two-phase sampling. Canadian Journal of Forest Research 43(5):441–449, DOI 10.1139/cjfr-2012-0381, URL <https://doi.org/10.1139/cjfr-2012-0381>
- Mandallaz D (2013b) A three-phase sampling extension of the generalized regression estimator with partially exhaustive information. Canadian Journal of Forest Research 44(4):383–388, DOI 10.1139/cjfr-2013-0449, URL <https://doi.org/10.1139/cjfr-2013-0449>

- Mandallaz D, Breschan J, Hill A (2013) New regression estimators in forest inventories with two-phase sampling and partially exhaustive information: a design-based monte carlo approach with applications to small-area estimation. *Canadian Journal of Forest Research* 43(11):1023–1031, DOI 10.1139/cjfr-2013-0181, URL <https://doi.org/10.1139/cjfr-2013-0181>
- Mandallaz D, Hill A, Massey A (2016) Design-based properties of some small-area estimators in forest inventory with two-phase sampling - revised version. Tech. rep., Department of Environmental Systems Science, ETH Zurich, DOI 10.3929/ethz-a-010579388, URL <https://doi.org/10.3929/ethz-a-010579388>
- Massey A, Mandallaz D, Lanz A (2014) Integrating remote sensing and past inventory data under the new annual design of the swiss national forest inventory using three-phase design-based regression estimation. *Canadian Journal of Forest Research* 44(10):1177–1186, DOI 10.1139/cjfr-2014-0152, URL <https://doi.org/10.1139/cjfr-2014-0152>
- Naesset E (2014) Area-based inventory in norway – from innovation to an operational reality. In: *Forest Applications of Airborne Laser Scanning - Concepts and Case Studies*, Springer, chap 11, pp 216–240, DOI 10.1007/978-94-017-8663-8
- Polley H, Schmitz F, Hennig P, Kroher F (2010) Germany. In: *National Forest Inventories - Pathways for Common Reporting*, Springer, chap 13, pp 223–243, DOI 10.1007/978-90-481-3233-1
- R Core Team (2017) R: A Language and Environment for Statistical Computing. R Foundation for Statistical Computing, Vienna, Austria, URL <https://www.R-project.org/>
- Rao JN (2015) Small-Area Estimation. Wiley Online Library
- Saborowski J, Marx A, Nagel J, Böckmann T (2010) Double sampling for stratification in periodic inventories—finite population approach. *Forest ecology and management* 260(10):1886–1895
- Särndal CE, Swensson B, Wretman J (2003) Model assisted survey sampling. Springer Science & Business Media
- Schmitz F, Polley H, Hennig P, Dunger K, Schwitzgebel F (2008) Die zweite Bundeswaldinventur - BWI2: Inventur- und Auswertmethoden, Bundesministerium für Ernährung, Landwirtschaft und Verbraucherschutz (Hrsg)
- Steinmann K, Mandallaz D, Ginzler C, Lanz A (2013) Small area estimations of proportion of forest and timber volume combining lidar data and stereo aerial images with terrestrial data. *Scandinavian journal of forest research* 28(4):373–385
- Stoffels J, Mader S, Hill J, Werner W, Ontrup G (2012) Satellite-based stand-wise forest cover type mapping using a spatially adaptive classification approach. *European journal of forest research* 131(4):1071–1089

- Stoffels J, Hill J, Sachtleber T, Mader S, Buddenbaum H, Stern O, Langshausen J, Dietz J, Ontrup G (2015) Satellite-based derivation of high-resolution forest information layers for operational forest management. *Forests* 6(6):1982–2013, DOI 10.3390/f6061982, URL <http://www.mdpi.com/1999-4907/6/6/1982>
- Thünen-Institut (2014) Dritte Bundeswaldinventur 2012. URL <https://bwi.info>, accessed: 2017-02-03
- White JC, Coops NC, Wulder MA, Vastaranta M, Hilker T, Tompalski P (2016) Remote sensing technologies for enhancing forest inventories: A review. *Canadian Journal of Remote Sensing* 42(5):619–641, DOI 10.1080/07038992.2016.1207484, URL <http://dx.doi.org/10.1080/07038992.2016.1207484>